Structure of the *O*-Acetylserine Sulfhydrylase Isoenzyme CysM from *Escherichia coli*[†,‡]

Michael T. Claus,[§] Georg E. Zocher,[§] Thomas H. P. Maier,[||] and Georg E. Schulz*[,§]

Institut für Organische Chemie und Biochemie, Albert-Ludwigs-Universität, Albertstrasse 21, D-79104 Freiburg im Breisgau, Germany, and Wacker-Chemie GmbH, Consortium für Elektrochemische Industrie, Zielstattstrasse 20, D-81379 München, Germany

Received March 16, 2005; Revised Manuscript Received May 4, 2005

ABSTRACT: The enzyme *O*-acetylserine sulfhydrylase participates in the biosynthesis of L-cysteine in bacteria and plants. The structure of isoenzyme B (CysM) from *Escherichia coli* was established in a hexagonal crystal form at 2.7 Å resolution (wild-type) and in a merohedrally twinned tetragonal crystal form at 2.1 Å resolution (surface mutant). Structural superpositions revealed the variations with respect to isoenzyme A (CysK) and explained the different substrate specificities. A geometric model of the reaction catalyzed by CysM is proposed. Both isoenzymes are used for the production of L-amino acid derivatives as building blocks for the synthesis of peptides and peptidomimetic drugs. Since the structure of CysM revealed a remarkable main chain variation at the active center, it constitutes a further starting point for engineering mutants with novel substrate specificities.

Cysteine is a standard amino acid that fulfills a crucial role in numerous cellular reactions. Moreover, cysteine forms disulfide bridges that fortify proteins outside the reductive milieu of the cytosol. The biosynthesis of cysteine follows two pathways: in bacteria, archaea, and plants, cysteine is produced from serine, whereas in higher animals, it is derived from methionine (*1*−*6*). The bacterial pathway starts with the *O*-acetylation of serine using acetyl-CoA, which is catalyzed by the enzyme serine acetyltransferase. The next step of this pathway is catalyzed by *O*-acetylserine sulfhydrylase (EC 2.5.1.47), eliminating acetate and adding hydrogen sulfide to produce cysteine (Figure 1) (*3*, *7*−*10*). This enzymatic function is expressed from the genes *cysK* and *cysM* as isoenzymes A (hereafter named CysK)[1] and B (CysM), which in *Escherichia coli* have 43% of their amino acid residues in common. The isoenzymes have different substrate specificities (*3*, *11*) which complement each other when adapting to a given growth condition. Sulfur is usually taken up as sulfate, which is then reduced to hydrogen sulfide accepted by both CysK and CysM. However, in the presence of thiosulfate, which is rejected by CysK, CysM is most helpful because it uses this substrate directly to form sulfocysteine that is easily converted to cysteine. When offered unnatural nucleophiles, both enzymes produce novel β-substituted L-amino acids to be applied as building blocks for the synthesis of pharmaceuticals and agrochemicals (*12*, *13*). In these syntheses the acceptance spectrum of CysM differs appreciably from that of CysK; in general, CysM

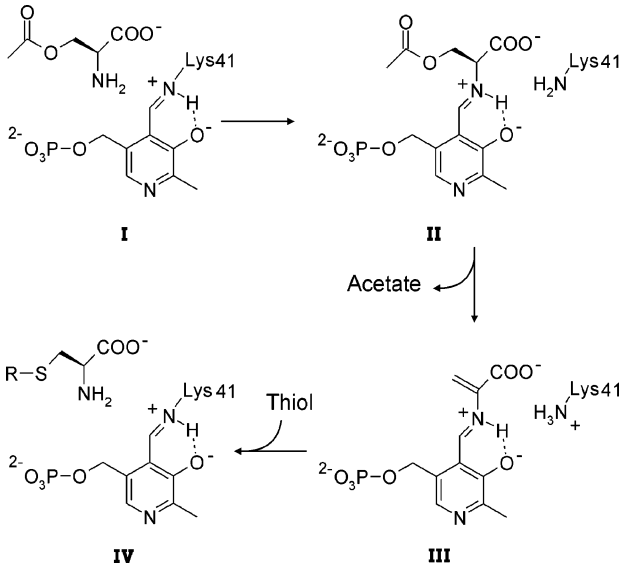

FIGURE 1: Reaction catalyzed by the *O*-acetylserine sulfhydrylases (*8*, *10*). In the standby state I, Lys41 forms a Schiff base with PLP. The incoming substrate exchanges with Lys41 to form an external aldimine with PLP (state II), which facilitates the elimination of acetate, creating an α-aminoacrylate intermediate (III). This intermediate is attacked by a nucleophile, which is usually a hydrogen sulfide resulting in cysteine (IV). However, both isoenzymes CysK and CysM may accept other nucleophiles producing unnatural L-amino acids (*12*).

† This work was supported by the Fonds der Chemischen Industrie and the Consortium für Elektrochemische Industrie.

‡ The atomic coordinates and structure factors are deposited in the Protein Data Bank as entries 2BHS and 2BHT.

* To whom correspondence should be addressed. Telephone: +49-761-203-6058. Fax: +49-761-203-6161. E-mail: georg.schulz@ocbc.uni-freiburg.de.

§ Albert-Ludwigs-Universität.

|| Wacker-Chemie GmbH.

[1] Abbreviations: *B*-factor, crystallographic temperature factor indicating flexibility; Cap, structural domain consisting of residues 1−10 and 35−142; Cap-$\beta\alpha\beta\alpha$, mobile part of Cap domain consisting of residues 85−134; Core, structural domain consisting of residues 11−34 and 143−294; CysK, *O*-acetylserine sulfhydrylase produced from the gene *cysK* of the cysteine operon, also named isoenzyme A; CysM, *O*-acetylserine sulfhydrylase produced from the gene *cysM* of the cysteine operon, also named isoenzyme B; CysM-rke, surface triple mutant E57R-Y148K-R184E of CysM; PLP, cofactor pyridoxal 5′-phosphate.

10.1021/bi050485+ CCC: $30.25
Published on Web 05/27/2005

Table 1: Data Collection[a]

		SeMet-labeled wild-type CysM				
	wild-type CysM	peak	edge	high remote	low remote	CysM-rke
space group	$P6_522$	$P6_522$	$P6_522$	$P6_522$	$P6_522$	$I4_1$ (twinned)
unit cell: $a = b$, c (Å)	195.6, 235.8	195.8, 234.3	195.8, 234.3	195.8, 234.3	195.8, 234.3	149.9, 193.9
wavelength (Å)	0.9795	0.9801	0.9804	0.9789	0.9831	0.8200
resolution (Å)	20−2.7 (2.84−2.67)	50−3.5 (3.6−3.5)	50−3.5 (3.6−3.5)	50−3.5 (3.6−3.5)	50−3.5 (3.6−3.5)	20−2.1 (2.16−2.10)
unique reflections	75225 (12562)	62645	63000	63003	62975	123872 (9986)
completeness (%)	99.4 (99.9)	98.9	99.4	99.4	99.4	99.8 (99.9)
multiplicity	16.6 (4.9)	5.8	5.9	5.9	5.8	3.9 (3.8)
I/σ_I	24.6 (3.9)	13.6 (4.6)	15.5 (6.5)	15.8 (5.9)	15.5 (5.4)	14.9 (3.5)
R_{sym-I} (%)	7.2 (38)	10.3 (41)	8.8 (30)	8.5 (32)	9.0 (37)	5.6 (39)
Wilson *B*-factor (Å^2)	76	58	58	60	59	35

[a] CysM is a homodimer in solution. The packing parameters of the hexagonal and tetragonal crystals were 4.9 and 4.2 Å^3/Da corresponding to 75% (v/v) and 70% (v/v) solvent, respectively, which is very spacious for soluble proteins (*38*). Both crystal forms contained four subunits per asymmetric unit. In the hexagonal crystals the axes of two dimers coincided with crystallographic 2-fold axes, and one dimer axis was local. The tetragonal crystals contained two local dimers per asymmetric unit. Values in parentheses refer to the outermost shell.

tends to accept larger substrates (*12*). Here, we present the structure of CysM from *E. coli*, compare it with CysK, and discuss the technological implications.

MATERIALS AND METHODS

The gene of CysM was expressed at 25 °C in *E. coli* BL21-(DE3) using vector pFL145 based on pASK-IBA3 (IBA, Göttingen). The culture medium was supplemented with pyridoxine. The harvested cells were sonicated and centrifuged, and the supernatant was applied to an anion-exchange column (Source 30Q, Amersham). The CysM-containing fractions were identified by SDS−PAGE and then incubated in 2 mM pyridoxal 5′-phosphate (PLP) at 4 °C for 4−6 h in order to achieve full PLP occupancy (*14*). The purification was continued with a further anion-exchange column (Source 15Q, Amersham) followed by gel filtration (Superdex-75, Amersham) and yielded about 60 mg of pure CysM/L of culture. The resulting PLP content was monitored using the A_{280}:A_{412} ratio, which showed occupancies around 96% (*15*). L-Selenomethionine-labeled CysM was produced by metabolic inhibition (*16*) and purified like the wild-type enzyme, except that 3 mM DTT was added to all buffers. Using the hanging drop method, crystals of wild-type and Se-labeled CysM grew at 20 °C within about 3 days to sizes of up to 400 × 100 × 100 μm^3. The drops contained 2 μL of a 10 mg/mL CysM solution mixed with 2 μL of reservoir buffer [100 mM sodium citrate, pH 5.6, 100 mM ammonium sulfate, 20% (w/v) PEG 4000]. The crystals were transferred in three steps to 31% (v/v) glycerol in reservoir buffer and flash-frozen to 100 K in a nitrogen gas stream.

CysM mutants were produced with the QuikChange kit (Stratagene) and expressed and purified like the wild-type enzyme. Among them, only the triple surface mutant E57R-Y148K-R184E (named CysM-rke) yielded suitable crystals. The hanging drops contained 2 μL of a 10 mg/mL CysM-rke solution mixed with 2 μL of reservoir buffer [100 mM Na-HEPES, pH 7.6, 150 mM $CaCl_2$, 28% (w/v) PEG 400]. Crystals grew within 2−3 weeks to dimensions of 220 × 160 × 160 μm^3, and the transfer to 100 K was performed as with the wild-type crystals.

All data were collected at beamline X06SA at the Swiss Light Source (Villigen, CH) and processed using programs XDS and XSCALE (*17*). Initial attempts to solve the structure of the hexagonal wild-type crystals by molecular replacement with AMORE (*18*) using various models based on the known structure of isoenzyme CysK (*8*) failed. Phases were determined with the multiwavelength anomalous diffraction method (*19*) using SHELXD (*20*), SHELXE (*21*), and SHARP (*22*). The structure was refined with REFMAC (*23*, *24*) and CNS (*25*). Water molecules were added with ARP_waters (*23*, *26*). Using the wild-type model, the structure of the tetragonal crystals of mutant CysM-rke was solved by molecular replacement with MOLREP (*23*, *27*) and RESOLVE (*28*). It was first refined with REFMAC. After detecting perfect merohedral twinning with DETWIN (*23*, *29*), the structure was further refined with SHELXL (*30*). Solvent-accessible surfaces were calculated with NACCESS (*31*). Figures were drawn using POVScript+ (*32*) and POVRAY (http://www.povray.org).

RESULTS AND DISCUSSION

Structure Determination. CysM from *E. coli* is a dimer. Each subunit has a mass of 32893 Da and consists of 303 amino acid residues and one PLP molecule forming an internal aldimine with Lys41. The enzyme was overexpressed in *E. coli*, purified, and crystallized. The only crystal form obtained with wild-type CysM was hexagonal, had a very large unit cell, and diffracted X-rays to medium resolution (Table 1). Extensive molecular replacement trials using models based on isoenzyme CysK (*8*) yielded merely two of the four CysM subunits in the asymmetric unit, presumably due to the large unit cell. Therefore, we introduced selenomethionines and collected multiwavelength anomalous diffraction data (Table 1). Altogether, 51 of the expected 52 selenium positions were identified with SHELXD and SHELXE (*20*, *21*) and used for phasing with SHARP (*22*). The correct enantiomorph was selected visually from electron density maps. The quality of the resulting electron density map is shown in Figure 2A. It sufficed to build a complete initial model showing R_{cryst} and R_{free} values of 39% and 41%, respectively.

Using the wild-type data set, this model was then refined (Table 2). A sample showing the quality of the final phases is depicted in Figure 2B. The hexagonal crystals contained 48 CysM subunits organized as 24 symmetric dimers in the unit cell. Half of the dimers lay across crystallographic 2-fold axes while the other half contained local 2-fold axes. This corresponds to four CysM subunits per asymmetric unit.

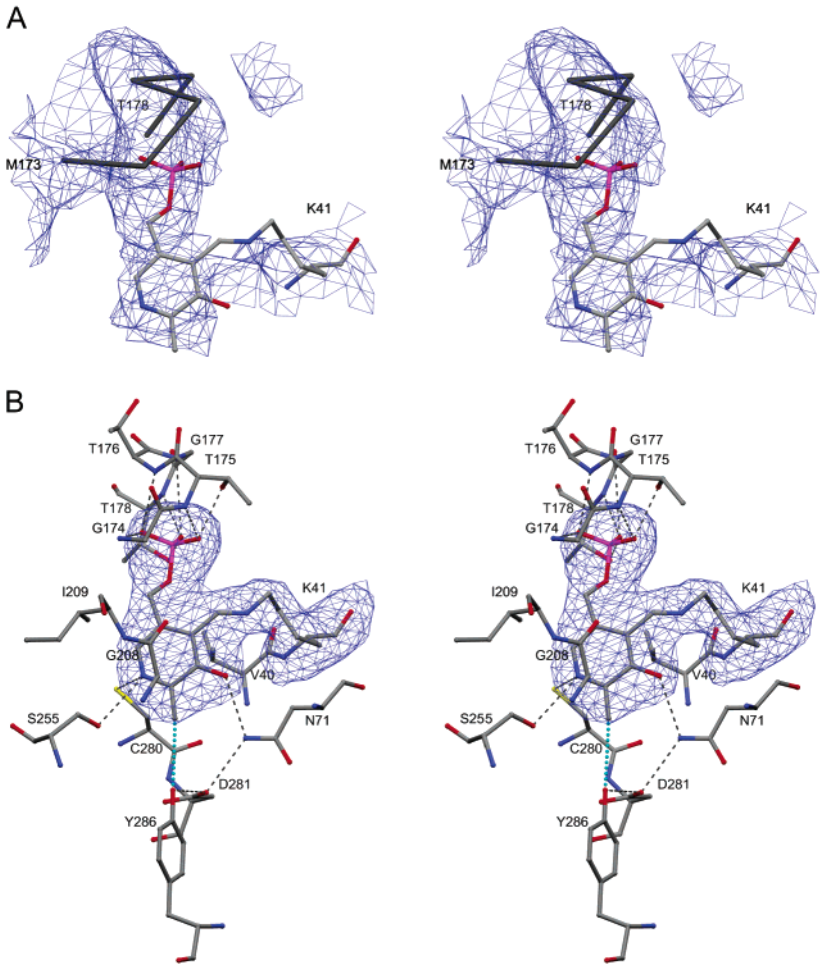

FIGURE 2: Stereoviews of electron density maps around PLP together with parts of the final refined model of the hexagonal crystals. (A) Electron density map at a contour level of 1σ based on the experimental phases to 3.5 Å resolution produced with SHARP (*22*). The model shows the internal aldimine and the Cα trace of residues 173−178. (B) $F_o - F_c$ electron density map at the 4σ contour level obtained with the final structure at 2.7 Å resolution after removing PLP and Lys41 and subsequent simulated annealing. All residues contacting PLP are included.

Table 2: Structural Refinement[a]

	wild-type	CysM-rke[b]
no. of atoms		
protein	8800	8701
PLP	60	60
water molecules	268	225
R_{cryst} (%)[c]	22.2 (32.6)	22.5 (29.1)
R_{free} (3% test set) (%)[c]	25.2 (35.7)	24.4
average *B*-factors (Å^2)		
protein	64	44[d]
PLP	51	35
water molecules	69	39[b]
rmsd bond lengths (Å)	0.014	0.010
rmsd bond angles (deg)	1.5	1.1
Ramachandran (*39*)		
allowed (%)	100.0	98.3
generously allowed (%)	0.0	1.5
disallowed (%)	0.0	0.2

[a] None of the crystals contained substrate analogues or inhibitors. [b] These crystals were perfect (50:50) merohedral twins and refined as such (*30*). Because twinning reduces the independence of observables, we limited the number of water molecules resulting in *B*-factors lower than the protein average. The comparatively high *R*-factors at 2.1 Å resolution are probably also caused by the twinning. [c] The numbers in parentheses refer to the outermost shell (not all are available). [d] The averages of subunits A and C were 40 Å^2 and those of subunits B and D 47 Å^2.

These four subunits resembled each other closely, showing an average Cα deviation of 0.3 Å and essentially identical *B*-factor distributions. The maximum deviation was 1.5 Å at helix α4. In all subunits residues 2−294 had defined conformations whereas residues 295−303 were invisible and therefore presumably mobile. The resulting dimer model is depicted in Figure 3A.

Since we intended to perform further structural analyses guiding engineering experiments, we tried to produce a crystal form that diffracted to higher resolution and hopefully also had a smaller unit cell, speeding up data acquisition. For this purpose we produced and tried to crystallize a total of 11 CysM mutants. All amino acid exchanges were on the surface distant from the active center and aimed to disturb a large packing contact of the hexagonal crystals. Eventually, the triple mutant CysM-rke yielded tetragonal crystals which diffracted to high resolution and appeared to belong to space group $I4_122$ (Table 1). The newly introduced Arg57 participated in one of the crystal contacts.

The structure of these crystals was established by molecular replacement using a CysM subunit from the hexagonal crystals. The structural refinement, however, halted at an R_{free} of about 36%. Revisiting the X-ray data, we detected that the crystals actually belonged to space group $I4_1$ and were perfectly twinned. Taking the twinning into account, the structure was then refined to good quality indices (Table 2). The tetragonal crystals contained four CysM subunits per

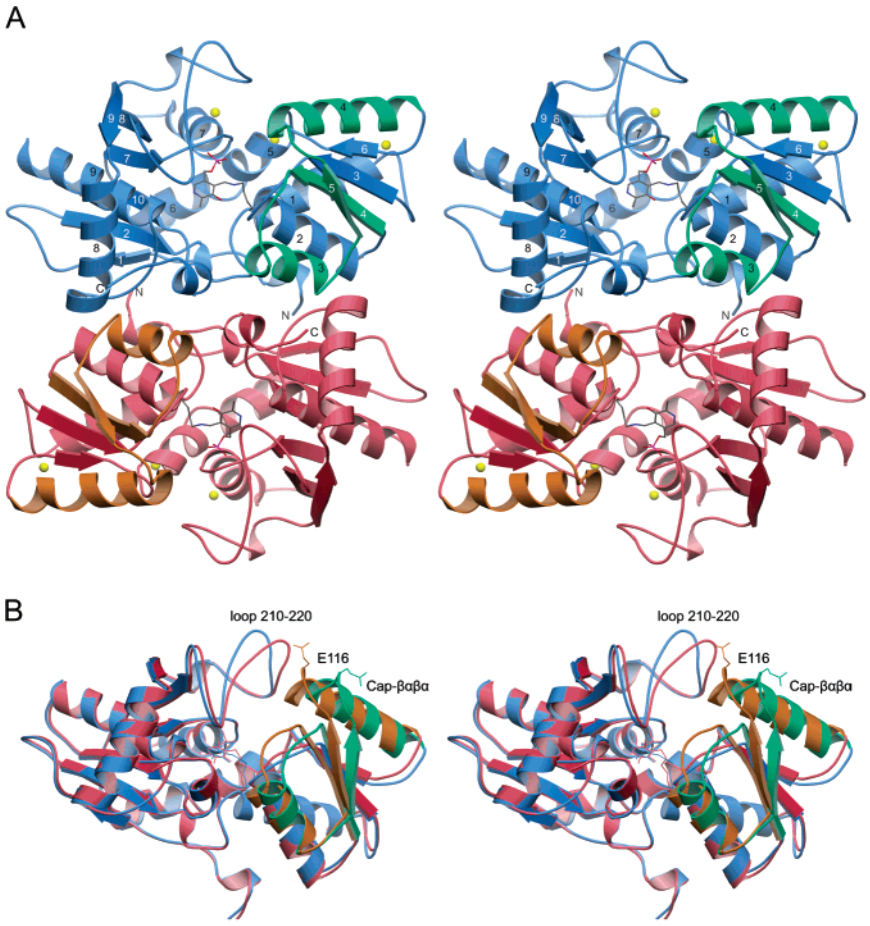

FIGURE 3: Stereo ribbon plots of CysM structures. (A) CysM dimer consisting of subunits A and B of the hexagonal crystals viewed along the molecular 2-fold axis. In the top subunit, the Core and the Cap domains are at the left- and right-hand sides, respectively. PLP bound to Lys41 is depicted as a ball-and-stick model located at the center. The Cap-$\beta\alpha\beta\alpha$ subdomains comprising residues 85−134 are marked by color differences. The secondary structures are detailed in Figure 4. The three surface mutations of CysM-rke are shown as yellow spheres far away from the active center. (B) Superposition of subunit A of the hexagonal crystals of wild-type CysM (blue and green, open conformation) with subunit A of the tetragonal crystals of CysM-rke (red and orange, closed conformation). The displacements at the active center involve the Cap-$\beta\alpha\beta\alpha$ subdomain and loop 210−220. Most likely they outline an induced fit on substrate binding.

asymmetric unit which were organized as dimers A−B and C−D. Subunits A and C were well-defined and virtually identical, whereas the others were more mobile so that residues 95−98, 112−119, and 125−127 of subunit B as well as residues 94−97 and 112−118 of subunit D could not be built. In all subunits the nine C-terminal residues were missing, as in the hexagonal crystals. A model of subunit A is depicted in Figure 3B in a comparison with the model from the hexagonal crystals.

Structure Description. All dimers in both crystal forms were clearly defined because they enclosed either a crystallographic or a local 2-fold axis. The dimer interface buries 1500 Å^2 solvent-accessible surface per subunit. The association energy derives mostly from a nonpolar patch between helix α3 of one subunit and the C-terminal 3_{10}-helix together with α8 from the other. The chain fold consists of ten β-strands, nine α-helices, and four 3_{10}-helices that are arranged in two domains which are referred to as Core and Cap domains (Figure 3A). The Core domain consists of residues 11−34 and 143−294 and has a central five-stranded parallel β-sheet (β2, β10, β7, β8, β9) with β1 as an antiparallel addition to one of the edges. This β-sheet is flanked by helices α5 through α9 and three 3_{10}-helices. The Cap domain contains residues 1−10 and 35−142 with a central four-stranded parallel β-sheet (β6, β3, β4, β5) flanked by helices α1 through α4 and the N-terminal 3_{10}-helix. The dimer interface involves both the Core and the Cap domains and all N and C termini (Figure 3A). Chain fold and dimerization of CysM resemble closely those of CysK (*8*, *9*, *33*−*35*). A structure-based sequence alignment of these isoenzymes is shown in Figure 4.

PLP forms an internal aldimine linkage to the ϵ-amino group of Lys41 from the Cap domain (Figure 2); it is fully occupied in both crystal forms in agreement with the A_{280}:A_{412} ratio of the crystallized protein. PLP is located in a pocket between the Core and the Cap domains (Figure 3). As shown in Figure 2B the cofactor ring is in hydrogen-bonding distance to the side chains of Asn71, Ser255, and Cys280 and makes nonpolar contacts to Val40, Gly174, Gly208, and Ile209. Ser255 and Cys280 may stabilize a partial negative charge at N1′. Conspicuously, there is a close 3.3 Å contact between the 2′-methyl group of PLP and the hydroxyl of Tyr286 that is hydrogen-bonded to Asp281. This arrangement may stabilize a partial positive charge at the 2′-methyl group. The phosphoryl group is tightly bound to the backbone of residues 174−178 at the N-terminal end of helix α7 carrying one or two negative charges. Such a phosphate-binding feature is rather common (*36*).

Segments 85−134 and 210−220 of all CysM subunits in both crystal forms show higher than average *B*-factors,

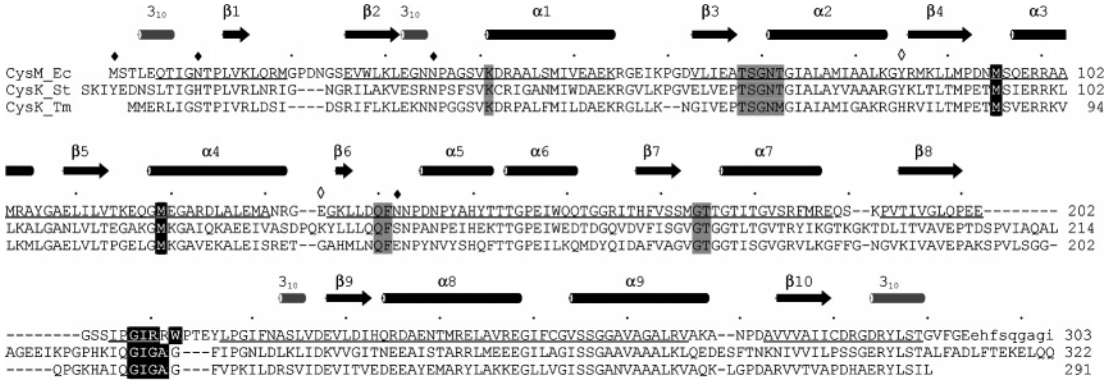

FIGURE 4: Structure-based sequence alignment of CysM (*E. coli*) with isoenzyme CysK from *S. typhimurium* (*33*) and CysK from *Th. maritima* (*35*). The underlying structure of CysM is from subunit A of the tetragonal crystals in the closed conformation. The CysK structures are also in closed conformations. The secondary structures are from CysM. The Cα atoms of the underlined residues of CysM are less than 3 Å apart from their counterparts in the other chains. Residues without structure are given in lower case letters. The borders of the Cap domain (♦) and of the Cap-$\beta\alpha\beta\alpha$ subdomain (◊) are marked. Residues lining the active center pocket are marked by a gray background (around *O*-acetylserine) and by black−white inversion (around the nucleophile). It should be noted that the known structure of CysK from *S. typhimurium* is virtually the same as that of CysK from *E. coli* because the sequences are 97% identical.

indicating segmental mobility. The first segment contains β4, α3, β5, and α4 of the Cap domain (here named Cap-$\beta\alpha\beta\alpha$), whereas the second is a long loop of the Core domain. In subunits B and D of the tetragonal crystals, Cap-$\beta\alpha\beta\alpha$ was so mobile that no structure could be assigned to 15 and 11 of its residues. For CysK, Cap-$\beta\alpha\beta\alpha$ was considered a flexible subdomain that assumed three positions named "open", "closed", and "inhibited" (*8*, *33*, *34*). Using these attributes, the crystal structure of CysK from *Thermotoga maritima* is in the closed conformation (*35*). Unfortunately, this structure lacks PLP and is therefore of only minor help in comparing the active centers. After the superposition of CysM with CysK (*8*, *33*) we found that the four CysM subunits in the hexagonal crystals were in the open conformation. In contrast, subunits A and C of the tetragonal CysM crystals were in the closed conformation, while the more mobile subunits B and D were nearer the open conformation.

The displacement between the open and the closed Cap-$\beta\alpha\beta\alpha$ subdomains of CysM is depicted in Figure 3B. It has a maximum of about 5 Å at Glu116. The inhibited conformation found in CysK (*34*) shows yet another Cap-$\beta\alpha\beta\alpha$ position, indicating that this subdomain is intrinsically mobile. Since CysM was crystallized without substrates or analogues, the two observed conformations are obviously determined by crystal packing forces. Actually, segment 109−117 of Cap-$\beta\alpha\beta\alpha$ is fixed by crystal contacts in the closed subunits A and C of the tetragonal crystals, whereas no such contact can be found in the more open subunits B or D. The four open subunits of the hexagonal crystals have other contacts. In light of multiple Cap-$\beta\alpha\beta\alpha$ conformations in CysM and CysK (*33*), we suggest that the observed open and closed positions outline an induced-fit movement performed on substrate binding.

Active Center. The active center is clearly defined by the covalently bound PLP at the bottom of the pocket between the Core and Cap domains (Figure 3). This pocket is lined by seven chain segments containing a total of 16 residues. These residues are marked in the sequence comparison between CysM and the two structurally known CysK isoenzymes (*8*, *35*) shown in Figure 4. Six of these segments are well conserved, while the seventh segment at positions 210−216 of CysM shows a decisive difference between CysM and CysK. CysM contains the large residues Arg210, Arg211, and Trp212 and a three-residue insertion, whereas CysK contains merely the small residues Gly230, Ala231, and Gly232. This local peculiarity, rather than any whole sequence or structure comparison, classifies the *Th. maritima* enzyme clearly as a CysK. It should be noted that the residues lining the common first substrate *O*-acetylserine are very well conserved while those lining the second substrate hydrogen sulfide differ greatly around Arg210. Considerable variations are also found on the outer rim of the active center pocket carrying Asn94, Lys115, and Ser205.

Because the closed conformations are relevant for the reaction geometry, they have been used in the superposition of CysM with CysK shown in Figure 5A. For CysK we took the structure of mutant Lys41→Ala that formed an external aldimine with a methionine (*33*). Methionine shows a steric resemblance to *O*-acetylserine and is therefore likely to reveal the actual substrate binding location, in particular, the position of the substrate carboxylate. On the basis of this structure, the steric limitations of the active center of CysK clearly define the position of an attacking hydrogen sulfide (Figure 5A). The same hydrogen sulfide position applies for CysM.

Residues 210−212 of CysK (CysM numbers) restrict the size of the nucleophile decisively. At this position, CysM has a three-residue insertion bulging toward the outside and thus enlarging the active center pocket in comparison to CysK. However, most of the additional space is filled by the side chain of Arg210 which most likely binds the substrate thiosulfate as shown in Figure 5B. The modeled α-aminoacrylate intermediate (state III of Figure 1) was sterically adjusted to the observed external aldimine of CysK (*33*). The carboxylate group of the substrate is accommodated by amide and hydroxyl dipoles of the peptide and forms a salt bridge to the detached Lys41. With these arrangements CysM is likely to catalyze the reaction in the same way as proposed for CysK (Figure 1).

The outward bulge of the main chain at position 210 of CysM enlarges the active center pocket compared to CysK. In our structure, this bulge is filled by the side chain of Arg210 which, however, can rotate away. This agrees with the observation that CysM tends to accept larger nucleophiles

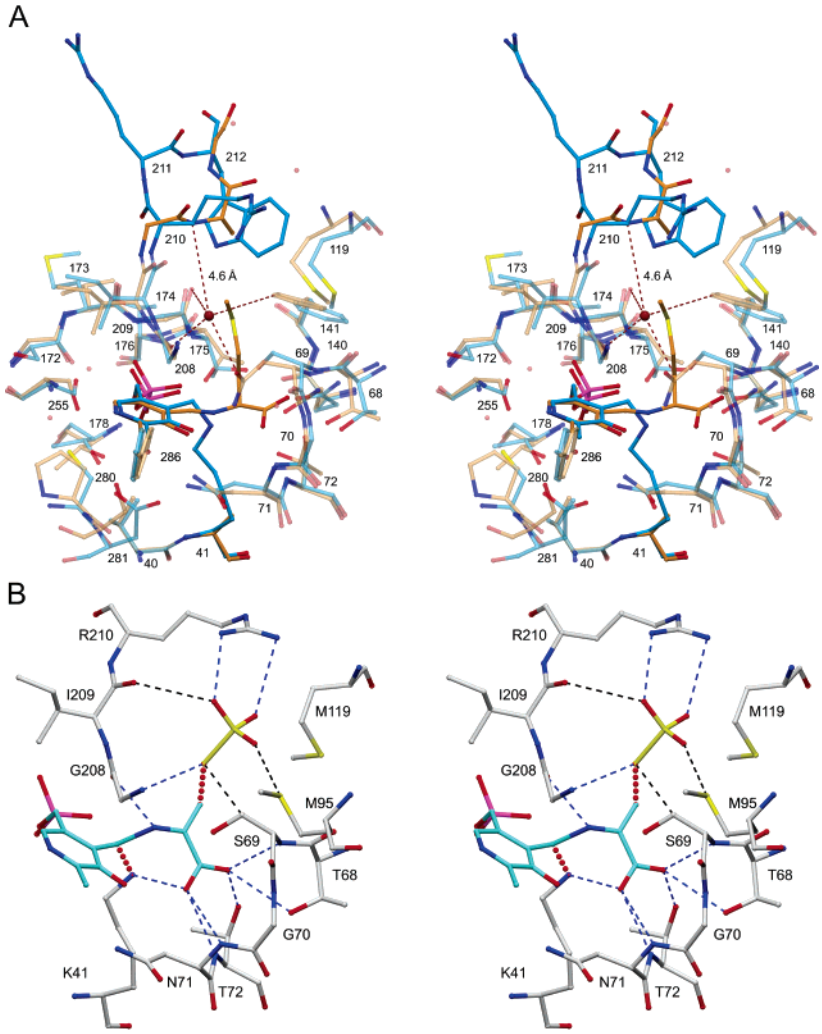

FIGURE 5: Stereoviews of the active centers of CysM and CysK in their closed conformations. (A) Subunit A of CysM-rke in the tetragonal crystals (blue) superimposed on the Lys41→Ala mutant of CysK (orange) (*33*). The external aldimine between methionine and PLP in CysK indicates the substrate position. Resembling parts of the two isoenzymes are given in transparent colors whereas differing parts are shown in dark colors. All residue numbers refer to CysM. The position of hydrogen sulfide (red sphere) is modeled. (B) The active center of CysM with a model of the bound α-aminoacrylate intermediate (state III of Figure 1) and the nucleophile thiosulfate. The model is based on the internal aldimine geometry so that Lys41 is merely disconnected (red dots). Actually, the detached lysine should form a salt bridge to the incoming substrate carboxylate. The thiosulfate is well stabilized by Arg210 of CysM that is absent in CysK, explaining the rejection of thiosulfate by CysK.

than CysK (*12*). In any case the structural variation explains the different substrate spectra of CysM and CysK (*11*, *12*).

CONCLUSION

The *O*-acetylserine sulfhydrylases participate in a central anabolic pathway of bacteria, archaea, and plants. Several bacteria possess two isoenzymes, CysK and CysM, that complement each other in order to cope with different growth conditions. The reported structure of CysM reveals a decisive active center deviation from CysK that shows how CysM accepts thiosulfate and thus avoids the sulfate-to-sulfide reduction usually required for cysteine biosynthesis. CysM has been applied for the production of unnatural L-amino acids from *O*-acetylserine which are versatile building blocks in the syntheses of pharmaceuticals and agrochemicals. The drug Viracept inhibiting HIV-protease, for instance, contains *S*-phenyl-L-cysteine (*37*) that is better produced with CysM than with CysK (*12*). Further drugs may follow. Since CysM and CysK have various side chains lining the active center, mutations should give rise to a future tool box of enzymes accepting numerous nucleophiles. For the pursuit of such endeavors, the main chain peculiarity around residue 210 of CysM provides a new starting point, which should appreciably increase the available spectrum of unnatural L-amino acids.

ACKNOWLEDGMENT

We thank G. Wich for discussions, K. Schwarz-Herion for his contribution during the initial stage of the analysis, and the team of the Swiss Light Source (Villigen, CH) for their help with the data collection.

REFERENCES

1. Kredich, N. M. (1971) Regulation of L-cysteine biosynthesis in *Salmonella typhimurium*, *J. Biol. Chem. 246*, 3474−3484.
2. Cooper, A. J. L. (1983) Biochemistry of sulfur-containing amino acids, *Annu. Rev. Biochem. 52*, 187−222.
3. Kredich, N. M. (1996) Biosynthesis of cysteine, in *Escherichia coli* and *Salmonella typhimurium*: Cellular and Molecular Biology (Neidhard, F. C., Ed.) Vol. 2, pp 514−527, ASM Press, Washington, DC.

4. Borup, B., and Ferry, J. G. (2000) Cysteine biosynthesis in the Archaea: *Methanosarcina thermophila* utilizes *O*-acetylserine sulfhydrylase, *FEMS Microbiol. Lett. 189*, 205−210.
5. Mino, K., and Ishikawa, K. (2003) Characterization of a novel thermostable *O*-acetylserine sulfhydrylase from *Aeropyrum pernix* K1, *J. Bacteriol. 185*, 2277−2284.
6. Wirtz, M., Droux, M., and Hell, R. (2004) *O*-acetylserine (thiol) lyase: An enigmatic enzyme of plant cysteine biosynthesis revisited in *Arabidopsis thaliana*, *J. Exp. Bot. 55*, 1785−1798.
7. Cook, P. F., and Wedding, R. T. (1978) Cysteine synthetase from *Salmonella typhimurium* LT-2, *J. Biol. Chem. 253*, 7874−7879.
8. Burkhard, P., Rao, G. S. J., Hohenester, E., Schnackerz, K. D., Cook, P. F., and Jansonius, J. N. (1998) Three-dimensional structure of *O*-acetylserine sulfhydrylase from *Salmonella typhimurium*, *J. Mol. Biol. 283*, 121−133.
9. Tai, C. H., Burkhard, P., Gani, D., Jenn, T., Johnson, C., and Cook, P. F. (2001) Characterization of the allosteric anion-binding site of *O*-acetylserine sulfhydrylase, *Biochemistry 40*, 7446−7452.
10. Tai, C. H., and Cook, P. F. (2001) Pyridoxal 5′-phosphate-dependent α,*β*-elimination reactions: mechanism of *O*-acetylserine sulfhydrylase, *Acc. Chem. Res. 34*, 49−59.
11. Tai, C.-H., Nalabolu, S. R., Jacobson, T. M., Minter, D. E., and Cook, P. F. (1993) Kinetic mechanisms of the A and B isozymes of *O*-acetylserine sulfhydrylase from *Salmonella typhimurium* LT-2 using the natural and alternative reactants, *Biochemistry 32*, 6433−6442.
12. Maier, T. H. P. (2003) Semisynthetic production of unnatural L-α-amino acids by metabolic engineering of the cysteine biosynthetic pathway, *Nat. Biotechnol. 21*, 422−427.
13. Watkins, K. J. (2001) Peptides: A boom in the making, *Chem. Eng. News*, 11−15 (January 8).
14. Schnackerz, K. D., and Cook, P. F. (1995) Resolution of pyridoxal 5′-phosphate from *O*-acetylserine sulfhydrylase from *Salmonella typhimurium* and reconstitution of apoenzyme with cofactor and cofactor analogues as a probe of the cofactor binding site, *Arch. Biochem. Biophys. 324*, 71−77.
15. Hidalgo, C., Sevilla, J. M., Pineda, T., and Blazquez, M. (1994) Enolimine and geminaldiamine forms in the reaction of pyridoxal phosphate with ethylenediamine. An electrochemical and spectroscopic contribution, *J. Phys. Org. Chem. 7*, 227−233.
16. Doublie, S. (1997) Preparation of selenomethionyl proteins for phase determination, *Methods Enzymol. 276*, 523−530.
17. Kabsch, W. (1993) Automatic processing of rotation diffraction data from crystals of initially unknown symmetry and cell constants, *J. Appl. Crystallogr. 26*, 795−800.
18. Navaza, J. (1994) AMORE: an automated package for molecular replacement, *Acta Crystallogr. A50*, 157−163.
19. Hendrickson, W. A., Horton, J. R., and Le Master, D. M. (1990) Selenomethionyl proteins produced for analysis by multiwavelength anomalous diffraction (MAD): A vehicle for direct determination of three-dimensional structure, *EMBO J. 9*, 1665−1672.
20. Schneider, T. R., and Sheldrick, G. M. (2002) Substructure solution with SHELXD, *Acta Crystallogr. D58*, 1772−1779.
21. Sheldrick, G. M. (2002) Macromolecular phasing with SHELXE, *Z. Kristallogr. 217*, 644−650.
22. de La Fortelle, E., and Bricogne, G. (1997) Maximum-likelihood heavy atom parameter refinement for multiple isomorphous replacement and multiwavelength anomalous diffraction methods, *Methods Enzymol. 276*, 472−494.
23. CCP4, Collaborative Computational Project, Number 4 (1994) The CCP4 suite: programs for protein crystallography, *Acta Crystallogr. D50*, 760−763.
24. Murshudov, G. N., Vagin, A. A., and Dodson, E. J. (1997) Refinement of macromolecular structures by the maximum likelihood method, *Acta Crystallogr. D53*, 240−255.
25. Brünger, A. T., Adams, P. D., Clore, G. M., DeLano, W. L., Gros, P., Grosse-Kunstleve, R. W., Jiang, J.-S., Kuszewski, J., Nilges, N., Pannu, N. S., et al. (1998) Crystallography and NMR system (CNS): A new software system for macromolecular structure determination, *Acta Crystallogr. D54*, 905−921.
26. Perrakis, A., Sixma, T. K., Wilson, K. S., and Lamzin, V. S. (1997) wARP: Improvement and extension of crystallographic phases by weighted averaging of multiple-refined dummy atomic models, *Acta Crystallogr. D53*, 448−455.
27. Vagin, A., and Teplyakov, A. (1997) MOLREP: an automated program for molecular replacement, *J. Appl. Crystallogr. 30*, 1022−1025.
28. Terwilliger, T. C. (2002) Automated main-chain model-building by template-matching and iterative fragment extension, *Acta Crystallogr. D59*, 34−44.
29. Yeates, T. O. (1997) Detecting and overcoming crystal twinning, *Methods Enzymol. 276*, 344−358.
30. Sheldrick, G. M. (1998) SHELX: Applications to macromolecules, in *Direct methods for solving macromolecular structures* (Fortier, S., Ed.) pp 401−411, Kluwer, Dordrecht, The Netherlands.
31. Hubbard, S. J., and Thornton, J. M. (1993) NACCESS computer program, Department of Biochemistry and Molecular Biology, University College, London, U.K.
32. Fenn, T. D., Ringe, D., and Petsko, G. A. (2003) POVScript+: a program for model and data visualization using persistence of vision ray-tracing, *J. Appl. Crystallogr. 36*, 944−947.
33. Burkhard, P., Tai, C.-H., Ristoph, C. M., Cook, P. F., and Jansonius, J. N. (1999) Ligand binding induces a large conformational change in *O*-acetylserine sulfhydrylase from *Salmonella typhimurium*, *J. Mol. Biol. 291*, 941−953.
34. Burkhard, P., Tai, C.-H., Jansonius, J. N., and Cook, P. F. (2000) Identification of an allosteric anion-binding site on *O*-acetylserine sulfhydrylase: Structure of the enzyme with chloride bound, *J. Mol. Biol. 303*, 279−286.
35. Heine, A., Canaves, J. M., von Delft, F., Brinen, L. S., Dai, X., Deacon A. M., Elsliger, M. A., Eshaghi, S., Floyd, R., Godzik, A., Grittini, C., Grzechnik, S. K., Guda, C., Jaroszewski, L., Karlak, C., Klock, H. E., Koesema, E., Kovarik, J. S., Kreusch, A., Kuhn, P., Lesley, S. A., McMullan, D., McPhillips, T. M., Miller, M. A., Miller, M. D., Morse, A., Moy, K., Ouyang, J., Page, R., Robb, A., Rodrigues, K., Schwarzenbacher, R., Selby, T. L., Spraggon, G., Stevens, R. C., van den Bedem, H., Velasquez, J., Vincent, J., Wang, X., West, B., Wolf, G., Hodgson, K. O., Wooley, J., and Wilson, I. A. (2004) Crystal structure of O-acetylserine sulfhydrylase (TM0665) from *Thermotoga maritima* at 1.8 Å resolution, *Proteins: Struct., Funct., Genet. 56*, 387−391.
36. Schulz, G. E. (1992) Binding of nucleotides by proteins, *Curr. Opin. Struct. Biol. 2*, 61−67.
37. Kaldor, S. W., Kalish, V. J., Davies II, J. F., Shetty, B. V., Fritz, J. E., Appelt, K., Burgess, J. A., Campanale, K. M., Chirgadze, N. Y., Clawson, D. K., Dressmann, B. A., Hatch, S. D., Khalil, D. A., Kosa, M. B., Lubbehusen, P. P., Muesing, M. A., Patrick, A. K., Reich, S. H., Su, K. S., and Tatlock, J. H. (1997) Viracept (Nelfinavir Mesylate, AG1343): a potent, orally bioavailable inhibitor of HIV-1 protease, *J. Med. Chem. 40*, 3979−3985.
38. Kantardjieff, K. A., and Rupp, B. (2003) Matthews coefficient probabilities: improved estimates for unit cell contents of proteins, DNA, and protein-nucleic acid complex crystals, *Protein Sci. 12*, 1865−1871.
39. Laskowski, R. A., MacArthur, M. W., Moss, D. S., and Thornton J. M. (1993) PROCHECK: a program to check the stereochemical quality of protein structures, *J. Appl. Crystallogr. 26*, 283−291.

BI050485+